# Using the Sonification for Hardly Detectable Details in Medical Images

**Veturia Chiroiu [a,*], Ligia Munteanu [a], Rodica Ioan [a,b], Ciprian Dragne [a], Cristian Rugină [a], Luciana Majercsik [c]**

[a] Institute of Solid Mechanics of Romanian Academy, Dept. of Deformable Media and Ultrasonics, Ctin Mille 15, Bucharest 010141
Emails: veturiachiroiu@yahoo.com, ligia_munteanu@hotmail.com, ciprian_dragne@yahoo.com, rugina.cristian@gmail.com

[b] University Spiru Haret, Bucharest, Dept. of Mathematics, 13 Str. Ion Ghica, Bucharest 030045, Romania, Email: rodicaioan08@yahoo.com,

[c] University Transilvania of Brasov, B-dul Eroilor nr. 29, Brașov 500036, Email: luciana.majercsik@gmail.com

DOI: 10.29322/IJSRP.9.07.2019.p9146
http://dx.doi.org/10.29322/IJSRP.9.07.2019.p9146

***Abstract***- In this paper, **t**h**e** inverse sonification problem is analysed in order to capture hardly detectable details in a medical image. The direct sonification problem is converting the data points into audio specimens by a transformation which involves data, acoustics parameters and sound representations. The inverse problem is reversing back the audio specimens into data points. By using the current sonification operator, the inverse approach does not bring any improvement in the medical picture after sonification. The obtained image is the same with the original one and does not bring additional information for diagnosis and surgical operation. In order to discover new details in a medical image, a new operator is introduced in this paper, by using the Burgers equation of sound propagation. The improving of the medical image is useful in interpreting the medical details in the tumour surgery. The inverse approach is exercised on several medical images.

***Index Terms***- Sonification; Burgers equation; Visualization tools; Laparoscopic surgery.

## I. Introduction

A major effort was devoted in the last years to enhance the quality of medical images used to surgery [1]. Since Roentgen's discovery of X-rays (1895) the medical imaging is constantly developing. The computed tomography, magnetic resonance imaging, nuclear imaging, and ultrasound-positioned medical imaging were implemented for medical purposes including to diagnoses and surgery.

To our knowledge, we are the first to apply the sonification theory to detect hidden details in medical images, such as vessels or tumors that cannot be directly seen with the eye.

The sonification theory was founded in 1952 by Pollack who applied the information theory to visualize the auditory displays [2, 3]. The first International Community for Auditory Display Conference (ICAD) organized by Kramer in 1992 discusses different issues ranging from the sciences and technology to the arts [4, 5]. Licht traces in 2007 the history of the sound art by highlighting the old art such as Sonic Youth and the contemporary art that led to interesting applications [6].

The nano-guitar built by Cornell University physicists from the crystalline silicon no larger than a single human blood cell, invites the bacteria inside a person to play and thus to be easily detected and tracked with a stethoscope [7]. The quantum whistle is a nano-scale sound which is able to discover vibrations in superfluid gases that are predicted by quantum theory [8].

The sonification theory introduces new insights into illnesses such as the Alzheimers's dementia [9] and trauma of the body motions such as walking, turning, rising arms or legs [10]. The sonification of images is less studied so far to our knowledge. This is because the applying of current sonification operator in the inverse approach does not bring any improvement in the medical image. The sonification operator is based on the linear theory of sound motion.

This paper introduces a new sonification operator based on the Burger nonlinear theory of the sound propagation. The new operator is capable to solve the inverse sonification problem and to improve the content of the medical image.

The paper is organized as follows: Section 2 is devoted to description of the direct problem of sonification. A description of the new sonification operator based on the Burgers equation of sound propagation is presented in Section 3. The applications are presented in Section 4, and Section 5 contains Conclusions.

## II. DIRECT PROBLEM OF SONIFICATION

The direct problem of sonification is well known in the literature [11-14]. The sonification operator $S^0$ maps the point data $D$ into audio samples $Y^0$ $S^0 : D \to Y^0$, $S^0 : x(t) \to y^0(t^0, x(t), p^0)$, with $x(t)$ the 1D point data to be transformed into audio samples, $t$ is the data time, $t^0$ is the sonification time, and $p^0 \subseteq P^0$, $P^0 = \{k^0, \Delta^0, f_{ref}^0, \alpha^0, \beta^0, \phi^0, \varepsilon^0, g^0, \gamma^0, H^0\}$ are the sonification parameters: $k^0$ is the compression coefficient on the time interval $T^0 = T / k^0$, $\Delta^0 \geq 0$ is the dilation coefficient, $f_{ref}^0$ is the reference frequency, $\alpha^0, \beta^0 \geq 0$ are the pitch scaling parameters, $\phi^0 \geq 1$ is the power distortion coefficient, $\varepsilon^0 \geq 0$ is the amplitude's threshold, $g^0$ is the gain function, $\gamma^0$ is the decay coefficient and $H^0$ is the function of the timbral control.

The 1D data string $x(t)$ is divided into non-overlapping sections of different length. The variables of the data domain are $t, t_i, T$. The signal $x(t)$ is understood as a sequence $x(n)$ at the rate of sample $f_s$ in $T$ seconds. The $x(n)$ consists of $N = T \times f_s$ samples. The time points $t_i$ separate $x_i(t)$. If $t_0 = 0$ and $t_M = T$ a division in $M$ segments of $x_i(t)$ can be written as

$$x_i(t) = \begin{cases} x(t + t_{i-1}) & 0 \leq t \leq (t_i - t_{i-1}) \\ 0 & \text{else} \end{cases} \tag{1}$$

The duration of each segment is $T_i = t_i - t_{i-1}$ The segments $x_i(t)$ are sonified as a succession of events $y_i^0(t^0)$ which are be longer or shorter than $T_i$

$$y^0(t^0) = \sum_{i=1}^{M} y_i^0(t^0 - t_{i-1}^0),\ t_{i-1}^0 = \frac{t_{i-1}}{k^0}\ . \tag{2}$$

The sonification signal $y^0(t^0)$ can be expressed as

$$y_i^0(t^0) = | x_i(\Delta^0 t^0) | \sin\left( 2\pi \int_0^{t^0} f_{ref}\, 2^{(x_{trend}(t_{i-1}) + x_i(\Delta^0 t^{0'}))}\, \mathrm{d}t^{0'} \right), \tag{3}$$

where $x_i(\Delta^0 t^{0'})$ is the mean free segment, and $x_{trend}(t_{i-1})$ is the trend signal at the starting point for pitch modulation. Parameter $\Delta^0$ gives the length of the acoustic event $T_i^0$. If $\Delta^0 = k^0$ the adjacent events do not overlap but for $\Delta^0 \leq k^0$ they overlap.

The operator $H^0$ is a sine function and introduces the control of timbre

$$y_i^0(t^0) = a_i(t^0) H^0 < \sin\left( 2\pi \int_0^{t^0} f_{ref}\, 2^{b_i(t^{0'})}\, \mathrm{d}t^{0'} \right) >, \quad b_i(t^{0'}) = \left( \alpha^0 x_{trend}(t_{i-1}) + \beta^0 x_i(\Delta t^{0'}) \right), \tag{4}$$

where $a_i(t^0)$ is the amplitude modulator, $f_{ref}$ is the base frequency for the pitch range of sonification and $b_i(t^0)$ is a pitch modulator. The amplitude modulator is

$$a_i(t^0) = | x_i(\Delta^0 t^0 |^{\phi^0}\ ,\ \phi^0 \geq 1, \tag{5}$$

where $\varphi^0$ is the amplitude modulator. A half-wave rectification is included for exceeding a threshold $\varepsilon^0$ around the mean of the amplitude

$$a_i(t^0) = g\left( | x_i(\Delta^0 t^0 |, \varepsilon^0 \right)\ ,\quad g(x, \varepsilon^0) = \begin{cases} x - \varepsilon^0 & x \geq \varepsilon^0 \\ 0 & \text{else} \end{cases} \tag{6}$$

## III. NEW SONIFICATION OPERATOR

The new sonification operator has the capability to bring gains in a medical image by discovering of hardly detectable details. We are looking for a new operator to replace (3) which is based on the linear theory of sound propagation. To introduce a new sonification operator, the Burgers equation of sound propagation is used.

Let us to consider a digital image $B$ of area $A$, seen as a collection of $N$ pixels $D = \{d_1, d_2, ..., d_N\}, d_i \in R^N$. The $B$ is subjected to external force $f(t)$ written as a sum of the excitation harmonic force $F_p(t)$ and the generation sound force $F_s(t)$. The last force is

introduced to build the sonification operator. The response of $B$ to $f(t)$ is a new configuration $b$ defined of all points $P \in B$ at the time $t$ resulting by vibration of $B$ . The vibration of $B$ is described by Burgers equation [15]

$$\frac{\partial v}{\partial x} - \frac{\beta}{c_0^2} v \frac{\partial v}{\partial \tau} - \frac{b}{2\rho_0 c_0^3} v \frac{\partial^2 v}{\partial \tau^2} = 0, \tag{7}$$

where $x = (x_1, x_2, x_3)$, $v = (v_1, v_2, v_3)$ is the vector of acoustic velocity, $\tau = t - x/c_0$ is the retarded time, $t$ is time, $c_0$ is the velocity of sound in the linear approximation, $b = (b_1, b_2, b_3)$ are the dissipation coefficients, $\rho_0$ is density of medium, $\beta = (\beta_1, \beta_2, \beta_3)$ is nonlinearity coefficient. Details on the propagation of waves in nonlinear 1D media can be found in [16-19]

Equation (7) admits the cnoidal solutions [20]. These solutions are expressed in terms of the Jacobi elliptic functions (cnoidal solutions) or the hyperbolic functions (solitons).

Given a known force $F_p$ , we determine the unknown force $F_s$ such that the acoustic power radiated from $B$ to be minimum. The acoustic power radiated from $B$ is

$$W = \frac{A}{2} v^T p, \tag{8}$$

where $v$ is the velocity verifying (7) and $p$ the acoustic pressure vector, $A$ is the area of the rectangular photo, and the subscript $T$ means the transpose [21].

We suppose that the solutions $v_i$, $i = 1,2,3$ of (7) are expressed as

$$v_i = \sum_{j=1}^{l} a_j \mathrm{cn}^j(m_i, \eta_i) + \frac{\sum_{j=1}^{l} b_j \mathrm{cn}^j(m_i, \eta_i)}{1 + \sum_{j=1}^{l} c_j \mathrm{cn}^j(m_i, \eta_i)}, \quad i = 1,2,3, \tag{9}$$

where $\eta_i = k_{1i}x_1 + k_{2i}x_2 + k_{3i}x_3 - \omega_i t + \tilde{\phi}_i$, $l$ is a finite number of degree of freedom of the cnoidal functions, $0 \le m \le 1$ is the moduli of the Jacobean elliptic function, $\omega$ is frequency and $\tilde{\phi}$ the phase, $k_1, k_2, k_3$ are components of the wave vector [20]. In the following we stop to $l = 2$ , and we will see that there are no sensible improvements in solutions for $l > 2$ By setting

$$\frac{\partial W}{\partial F_s} = 0 \ , \tag{10}$$

the function $F_s(t)$ is determined.

The unknown parameters $P_j = \{m_j, \omega_j, k_{1j}, k_{2j}, k_{3j}, \tilde{\phi}_j, a_1, b_1, c_1, a_2, b_2, c_2\}$, $j = 1,2,3$, are evaluated by a genetic algorithm. The objective function $\Upsilon(P_j)$ to be minimized is written with respect to residuals of (7) and (10)

$$\Upsilon(P_j) = 3^{-1} \sum_{j=1}^{3} \delta_{1j}^2 + \delta_2^2, \tag{11}$$

with

$$\delta_{1j} = \frac{\partial v_j}{\partial x_j} - \frac{\beta_j}{c_0^2} v_j \frac{\partial v_j}{\partial \tau} - \frac{b_j}{2\rho_0 c_0^3} v_j \frac{\partial^2 v_j}{\partial \tau^2}, \quad \delta_2 = \frac{\partial W}{\partial F_s}. \tag{12}$$

The genetic algorithm is running until it is reached a non-trivial minimizer, which will be a point at which (11) admits a global minimum.

The quality of results depends on the values of $\Upsilon$ . The required precision is taken to be six places after the decimal point. The following parameters are considered: number of populations 200, the reproduction ratio 1.0, multi-point crossover number 1, probability of mutation 0.5, and maximum number of generations 500.

The sonification operator $S$ is written with respect to $F_s$

$$S(D,t) = F_s(\tilde{D},t) + \frac{F_s(\tilde{D},t)}{1 + F_s(\tilde{D},t)}, \tag{13}$$

with $D = \{d_1, d_2, ..., d_N\}, d_i \in R^N$ is the original image data domain, $\tilde{D} = \{\tilde{d}_1, \tilde{d}_2, ..., \tilde{d}_N\}, \tilde{d}_i \in R^N$ is the domain of point data in the sonified image, and $t$ is the sonification time. Data $D$ is arranged under a matrix with arbitrarily number of elements. This matrix is

shown in Fig.1a. The elements of the matrix contain interfaces or borders between the colors and nuances, lines and curved lines (Fig.1b).

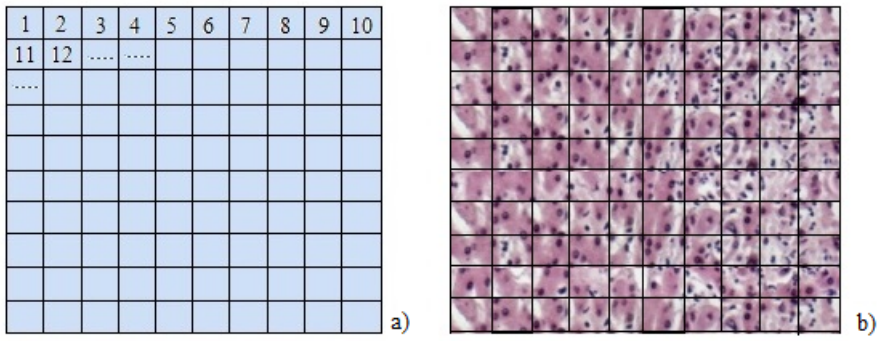


Fig.1. a) Matrix of data with arbitrarily number of elements. b) An image with borders separating the colors and nuances, lines and curved lines, etc.

The sharp interface conditions for which the matching of displacements and stresses at the image interfaces is imposed for (7). The reflections by the edges are removed by Dirichlet and Neumann boundary conditions. The reflection coefficient is [22]

$$r_j = \left( \frac{1-\cos\theta}{1+\cos\theta} \right)^j , \tag{14}$$

where $j$ is the degree of approximation, and $\theta$ is the incidence angle. The reflections from boundaries are removed by coupling the Dirichlet fixed boundary conditions solution to the Neumann free boundary conditions solution. For more than one component of displacement, the Dirichlet and Neumann conditions alternate components at the boundaries. When more than one boundary is nonreflecting, more solutions are added to eliminate multiple reflections.

The blank spaces in the sonified image are filled through continuity by the solutions in the vicinity of interfaces and edges. The mapped data after sonification is typically containing the small blurred area, cavities and white dots due to the inaccuracies of the original medical images. These areas are filled with color and geometric lines, through continuity of the adjacent areas, so that the final image may contain new elements, new details that do not appear in the original image.

New inverse sonification technique was highlighted on some medical images used to surgical operations. In the next Section we present the applications.

## IV. APPLICATIONS

The medical images chosen for sonification represent different tissue samples with abrupt changes in profile. A 3D sample of a fictive rat liver is shown in Fig. 2a, and the size of constituents are shown in Fig. 2b, respectively. The rat liver involves severe disturbances zones between 10 and 50 $\mu m$ at the microscopic scale [23].

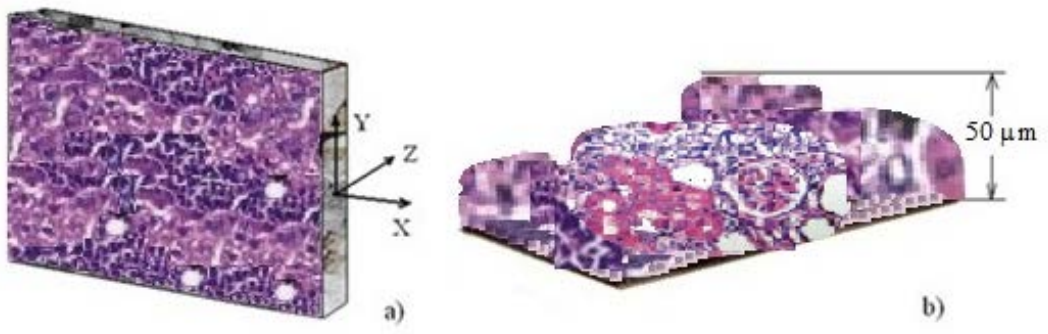


Fig. 2. a) A rat liver 3D sample; b) Size of constituents.

The sonification operator (14) is applied on different fictive images of fibrotic rat liver inspired from a study of effects of ginkgo biloba leaf extract against hepatic toxicity induced by methotrexate in rat [23, 24]. The images of cross-sections of the rat liver are

shown in Fig. 3. Fig. 4 visualizes the new images obtained by applying the sonification operator. A comparison of the images to the original ones leads to some differences observed in the last six images (yellow).

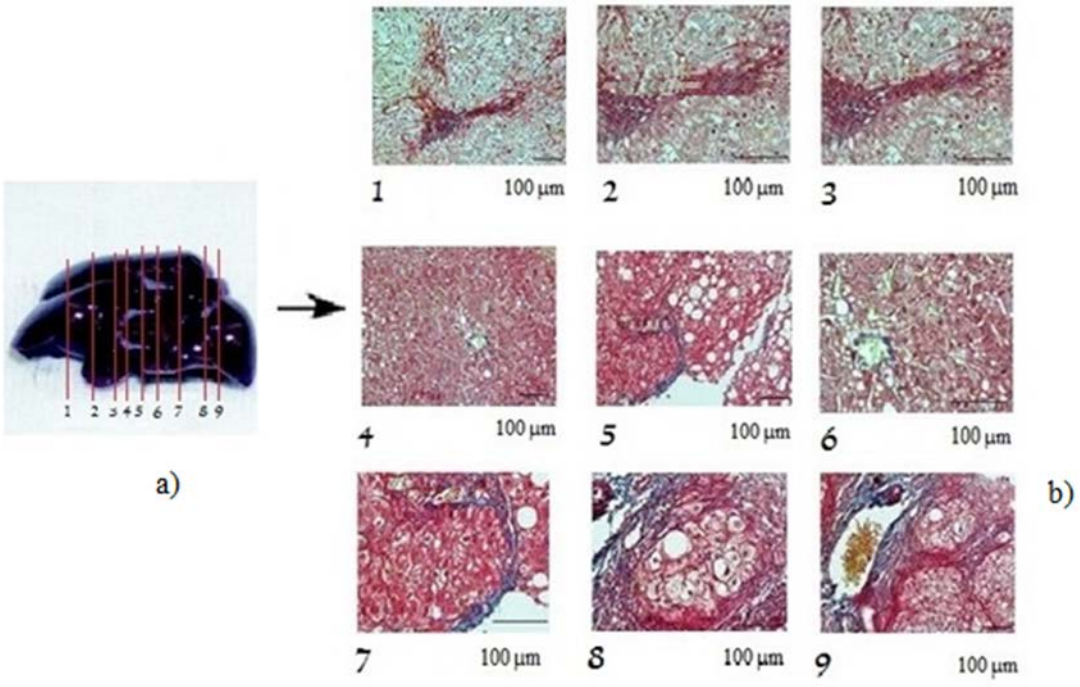


Fig. 3. Sectional slices of a rat liver sample; b) Cross-sectional slices of the sample.

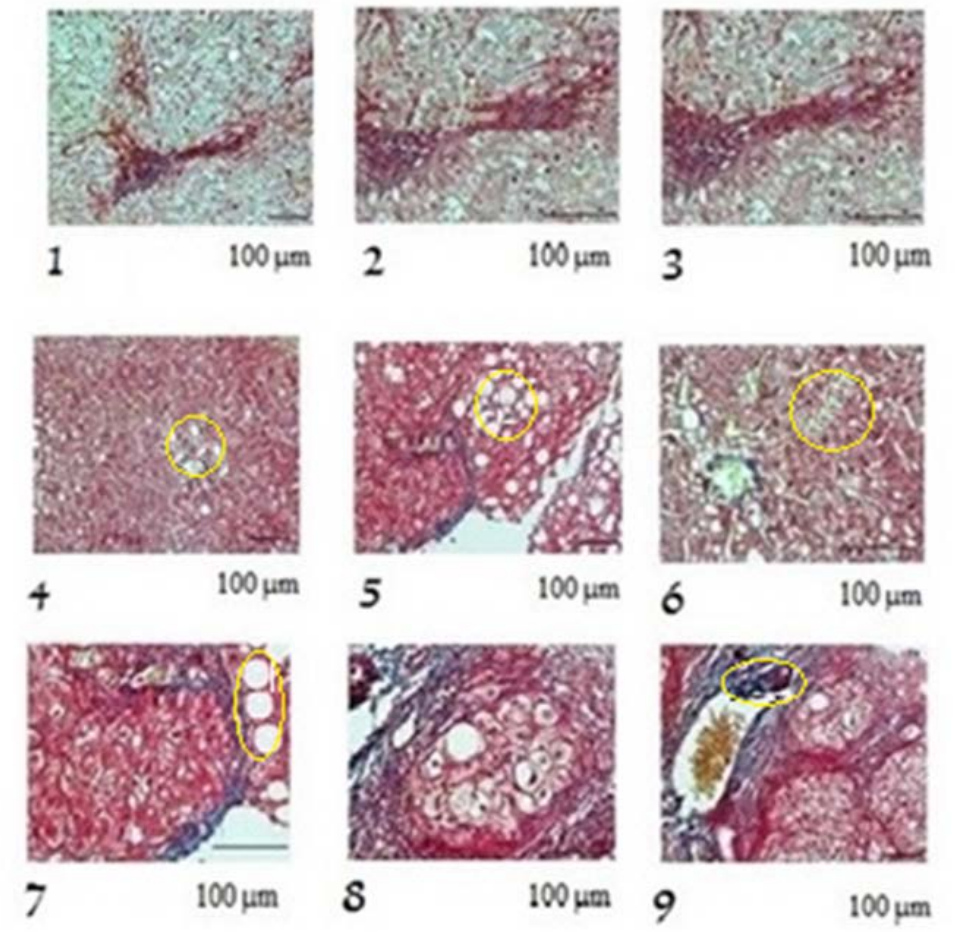


Fig. 4. Cross-sectional slices after sonification. Differences with original images are shown in yellow.

The work of Salameh [25] is considered next, related to the detection of nonalcoholic steatohepatitis in the fatty rat livers by magnetic resonance (MR) [26-28]. Fig. 5a shows the MR image of a liver rat with hepatocytes and strong hepatocellular. Details are purposefully hidden (red circles in Fig.5b). The inverse sonification operator recovered all initially hidden details (Fig.5c).

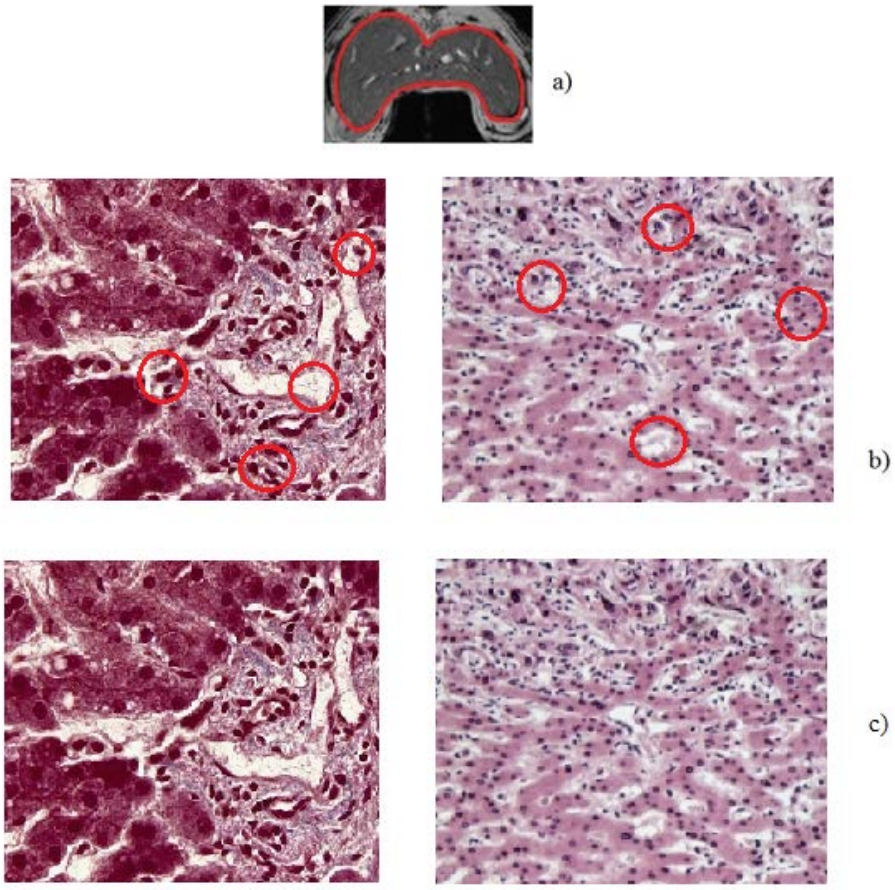


Fig. 5. a) A MR image of a rat liver; b) The initially hidden details were recovered by sonification technique.

Another exercise is related to the hepatic arterial chemotherapy [29-32], for which a catheter is inserted inside the gastroduodenal artery (GDA) to distribute the chemotherapy. A possible location of the hepatic arterial infusion catheter was discussed in [30]. Our exercise is to reobtain the CT image reported in this paper and presented in Fig.6. We intentionally spoil this image and apply to it apply the inverse sonification. The sonified image is shown in Fig.7d. This image is identically to the one of Fig.6.
Fig.7a shows the CT image of the hepatic artery (CHA- common hepatic artery, LHA - left hepatic artery, RHA - right hepatic artery, SA - splenic artery, Seg IV HA - segment IV hepatic artery) [30]. Fig. 7b shows the CT image of the left hepatic artery [30]. Fig. 7c shows the image we want to sonify.

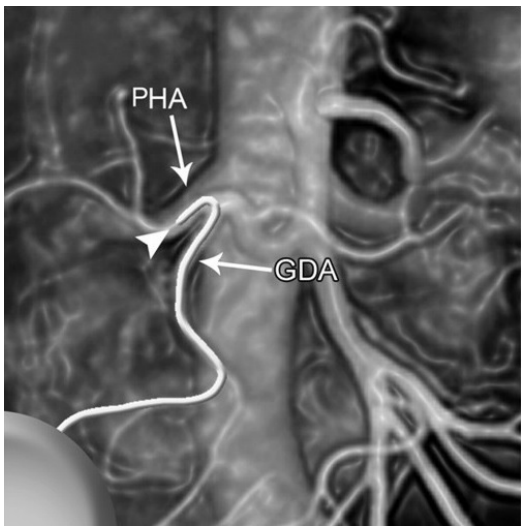

Fig. 6. A possible location of the hepatic arterial infusion catheter [30].

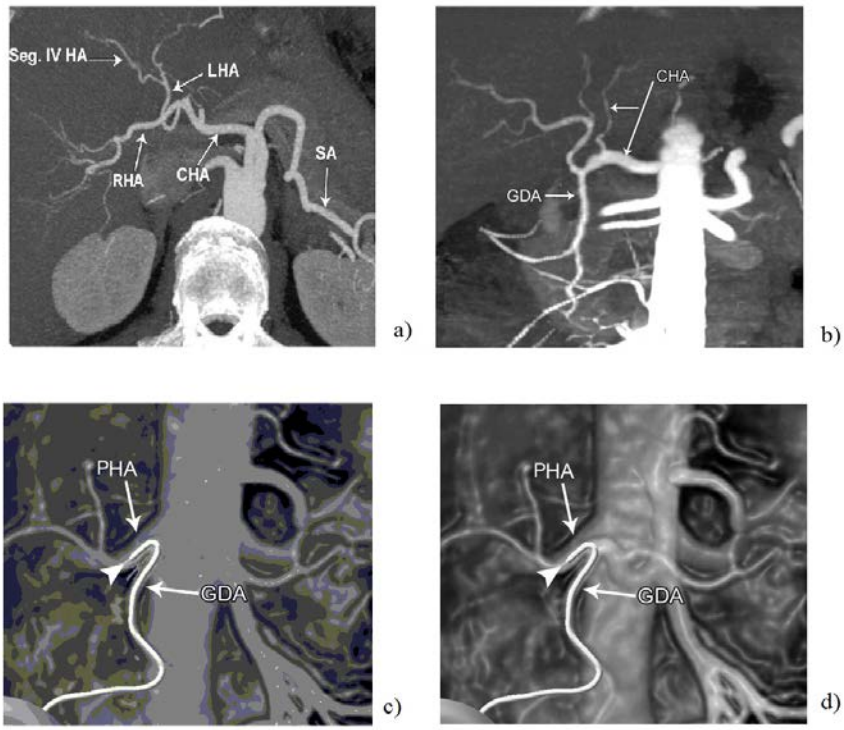


Fig. 7. a) CT image of the hepatic artery (CHA - common hepatic artery, LHA- left hepatic artery, RHA - right hepatic artery, SA - splenic artery, Seg IV HA - segment IV hepatic artery); b) CT image of the left hepatic artery; c) the image to be sonified; d) final sonified image.

The last exercise is the case of a tumor (pink color) located near the portal tree of the vascular branches (Fig. 8a) [33, 34]. The vascular territory (1) and the vessel branches in the vicinity of tumor (2) are shown in Fig. 8b. Three sonified images are obtained Fig. 9 for the frontal, caudal and cranial views. New details on the tumor are reported to surrounding area, and the shape and size of the tumor is better visualized.

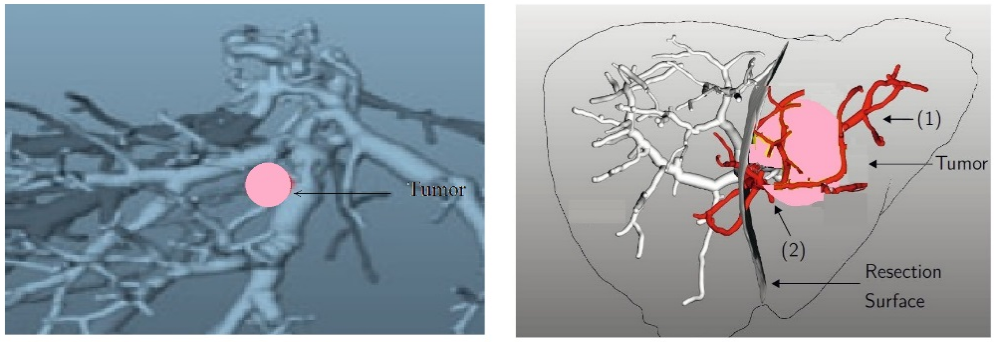


Fig. 8. a) The tumor location; b) Vascular map (1) and the vessel territory near the tumor (2).

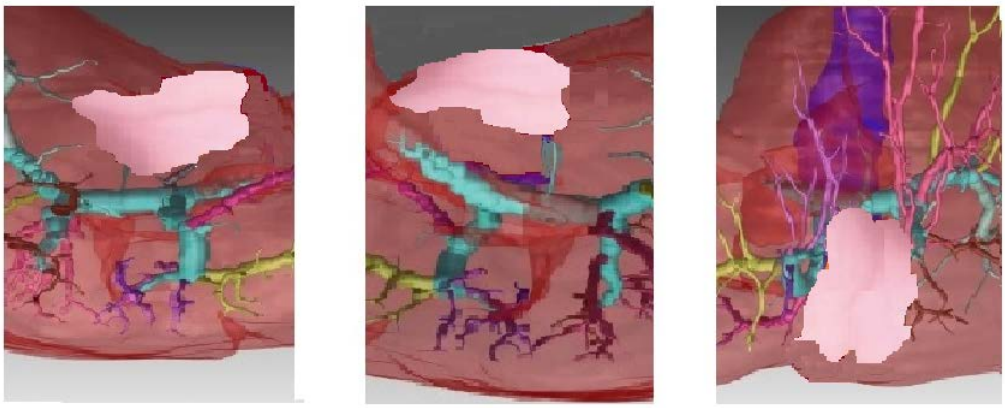

Fig. 9. New images in the vicinity of the tumor after sonification.

## V. CONCLUSIONS

A new sonification operator is proposed in this paper in order to convert the digital data into sound by using the cnoidal vibrations as a set of basic functions. By inverting the sound into image, the result highlights hidden details in the image seen by the sound and not seen by the eyes**.** To show the efficiency of the sonification algorithm and to verify the correctness of the results, we intentionally hide some details into the images. The new sonification operator has discovered the hidden details.

## ACKNOWLEDGMENT

This work was supported by a grant of the Romanian Ministry of Research and Innovation, CCCDI – UEFISCDI, project number PN-III-P1-1.2-PCCDI-2017-0221 / 59PCCDI/2018 (IMPROVE), within PNCDI III.

## REFERENCES

[1] Laal, M., Innovation Process in Medical Imaging, Procedia - Social and Behavioral Sciences, 81, 60-64 (2013).

[2] I. Pollack, The information of elementary auditory displays, Journal of the Acoustical Society of America, 24(6) 745-749 (1952).

[3] I. Pollack and L. Ficks, Information of elementary multidimensional auditory displays, Journal of the Acoustical Society of America, 26, 155-158 (1954).

[4] G. Kramer, An introduction to auditory display, In: Kramer G (eds) In auditory display, Addison-Wesley, Boston, MA, 1-79 (1994).

[5] G. Kramer, B. Walker, T. Bonebright, P. Cook, J. Flowers, N. Miner and J. Neuhoff, Sonification report: Status of the field and research agenda. Tech. Rep., International Community for Auditory Display (1999).

[6] S. Shelley, M. Alonso, J. Hollowoof, M. Pettitt, S. Sharples, D. Hermes and A. Kohlrausch, Interactive sonification of curve shape and curvature data, In Lecture Notes in Computer Science 5763, Haptic and Audio Interaction Design, 4th International Conference, HAID2009, Dresden, Germany, Sept 10-11, 2009 (eds. M. Ercan Altinsoy, Ute Jekosch, Stephen Brewster), 1-60 (2009).

[7] H. Craighead and Silicon Guitar, http://www.npr.org/news/tech/970724.guitar.html (1997).

[8] J.C. Davis and R. Packard, Quantum oscillations between two weakly coupled reservoirs of superfluid He-3, Nature July 31 (1997).

[9] L. Gionfrida and A. Roginska, A novel sonification approach to support the diagnosis of Alzheimer's dementia, Frontiers in Neurology, 8, Article 647 (2017).

[10] Asri Ag Ibrahim and Alter Jimat Embug, Sonification of 3D body movement using parameter mapping technique, International Conference on Information Techmology and Multimedia (ICIMU) November 18-20, Putrajaya, Malaysia, 385-389 (2014).

[11] T. Bonebright, P. Cook and J. H. Flowers, Sonification Report: Status of the Field and Research Agenda, Faculty Publications, Department of Psychology, Paper 444 (2010).

[12] R. Holdrich and K. Vogt, Augmented audification, in ICAD 15: Proceedings of the 21st International Conference on Auditory Display, K. Vogt, A. Andreopoulou, and V. Goudarzi, Eds. Graz, Austria: Institute of Electronic Music and Acoustics (IEM), University of Music and Performing Arts Graz (KUG), 102–108 (2015).

[13] P. Vickers and R. Holdrich, Direct segmented sonification of characteristic features of the data domain, preprint, Department of Computer and Information Sciences, Northumbria University, Newcastle upon Tyne, UK (2017).

[14] J. Rohrhuber, $S_0$ - Introducing sonification variables, in Super-Collider Symposium 2010, Berlin, pp. 1–8 (2010).

[15] I. Demin, S. Gurbatov, N. Pronchatov-Rubtsov, O. Rudenko and A. Krainov, The numerical simulation of propagation of intensive acoustic noise, Published by the Acoustical Society of America, Proceedings of Meetings on Acoustics, Vol. 19, 045075 (2013) .

[16] M. Scalerandi, P.P. Delsanto, C. Chiroiu and V. Chiroiu, Numerical simulation of pulse propagation in nonlinear 1-D media, Journal of the Acoustical Society of America, 106 (5), 2424-2430 (1999).

[17] R. A. Toupin and B. Bernstein, Sound waves in deformed perfectly elastical materials. Acoustoelastic effect, Journal of the Acoustical Society of America, 33, 216 (1961).

[18] G.V. Norton and J G. Novarini, Including dispersion and attenuation directly in the time domain for wave propagatiom in isotropic media, Journal of the Acoustical Society of America, 113, 3024-3031, 2003.

[19] G.V. Norton and R. D. Purrington, The Westervelt equation with viscous attenuation versus a causal propagation operator. A numerical comparison, Journal of Sound and Vibration, 327, 163-172, 2009.

[20] L. Munteanu and St.Donescu, Introduction to Soliton Theory: Applications to Mechanics, Book Series Fundamental Theories of Physics, vol.143, Kluwer Academic Publishers, Dordrecht, Boston, Springer Netherlands, 2004.

[21] Ji Lin and J. Stuart Bolton, Sound power radiation from a vibrating structure in terms of structure-dependent radiation modes, Journal of Sound and Vibration, 335, 245–260, (2015).

[22] E.Ruffino, and P.P.,Delsanto, Problems of accuracy and reliability in 2D LISA simulations, Computers and Mathematics with Applications, 38, 89-97, 1999.

[23] E.Tousson, Z.Atteya, Afaf EI-Atash and Ola I.Jeweely, Abrogation by ginkgo byloba leaf extract on hepatic and renal toxicity induced by methotrexate in rats, Journal of Cancer Research and Treatment, 2(3), 44-51 (2014).

[24] V. Chiroiu, C. Dragne and A. Gliozzi, On the trajectories control of a hybrid robot, ICMSAV201818, October 25-26, Brasov (2018).

[25] N.Salameh and B.Larat, Early detection of steatohepatitis in fatty rat liver by using MR elastography, Radiology, 253(1) (2009).

[26] C. Rugina and C. Stirbu, On the sonoelasticity and sonification imaging theories with application to cooperative surgery robots, ICMSAV201818, October 25-26, Brasov (2018).

[27] L. Munteanu, R. Ioan and L. Majercsik, On the computation and control of a robotic surgery hybrid system, ICMSAV201818, October 25-26, Brasov (2018).

[28] V. Chiroiu, L. Munteanu, C. Dragne, C. Stirbu, On the diferential dynamic logic model for hybrid systems, Acta Technica Napocensis - series: Applied Mathematics, Mechanics, and Engineering, 61(4) (2018).

[29] V.Chiroiu, L.Munteanu and C.Rugină, On the control of a cooperatively robotic system by using a hybrid logic algorithm, Proceedings of the Romanian Academy, series A: Mathematics, Physics, technical Sciences, Information Science, 19(4) ( 2018).

[30] A. C. Onofrio, H. S. Anandkumar, R.N. Uppot, P.F. Hahn, C.R. Ferrone and D. Sahani, Vascular and Biliary Variants in the Liver: Implications for Liver Surgery, RadioGraphicsVol. 28, No. 2 (2008).

[31] D. Sahani, A. Mehta, M. Blake, S. Prasad, G. Harris and S. Saini, Preoperative hepatic vascular evaluation with CT and MR angiography: implications for surgery, Radio Graphics, 24(5), 1367–1380 (2004).

[32] D. Sahani, S. Saini and S. Nichols, Using multidetector CT for preoperative vascular evaluation of liver neoplasms: technique and results. AJR Am. J. Roentgenol, 179(1), 53–59 (2002).

[30] H. Lang, M. Hindennach, A.Radtke and H.O. Peitgen, Virtual liver surgery: Computer-assisted operation planning in 3D liver model, chapter 5 in Recent Advances in liver surgery by Renzo Dionigi, Landes Bioscience Madame Curie Bioscience Data base (2009).

[31] R. Shamir, I. Tamir, E. Daboo, L. Joskowicz and Y. Shoshan, A Method for Planning Safe Trajectories in Image-Guided Keyhole Neurosurgery. In: Jiang T, Navab N, Pluim JW, Viergever M. Medical Image Computing and Computer-Assisted Intervention–MICCAI 2010. Lecture Notes in Computer Science. 6363, Springer Berlin Heidelberg (2010).

## AUTHORS

**Veturia Chiroiu** – PhD Mathematics, Institute of Solid Mechanics of Romanian Academy, Dept. of Deformable Media and Ultrasonics, Ctin Mille 15, Bucharest 010141
Email: veturiachiroiu@yahoo.com
**Ligia Munteanu** – PhD Mathematics, Institute of Solid Mechanics of Romanian Academy, Dept. of Deformable Media and Ultrasonics, Ctin Mille 15, Bucharest 010141
Email: ligia_munteanu@hotmail.com
**Rodica Ioan** – PhD Mathematics, Institute of Solid Mechanics of Romanian Academy, Dept. of Deformable Media and Ultrasonics, Ctin Mille 15, Bucharest 010141/ University Spiru Haret, Bucharest, Dept. of Mathematics, 13 Str. Ion Ghica, Bucharest 030045
Email: *rodicaioan08@yahoo.com*
**Ciprian Dragne** – Mechanical Engineer, Institute of Solid Mechanics of Romanian Academy, Dept. of Deformable Media and Ultrasonics, Ctin Mille 15, Bucharest 010141
Email*:* ciprian_dragne@yahoo.com
**Ioan Rugina** – PhD Engineering, Institute of Solid Mechanics of Romanian Academy, Dept. of Deformable Media and Ultrasonics, Ctin Mille 15, Bucharest 010141
Email: rugina.cristian@gmail.com
**Luciana Majercsik** – University Transilvania of Brasov, B-dul Eroilor nr. 29, Brașov 500036
Email: luciana.majercsik@gmail.com

**Correspondence Author** – Veturia Chiroiu PhD Mathematics, Institute of Solid Mechanics of Romanian Academy, Dept. of Deformable Media and Ultrasonics, Ctin Mille 15, Bucharest 010141
Email: veturiachiroiu@yahoo.com